Scientific Research Publishing

Journal of Geoscience and Environment Protection, 2022, 10, 354-372
https://www.scirp.org/journal/gep
ISSN Online: 2327-4344
ISSN Print: 2327-4336

Urban Heat Island and Land Use/Cover Dynamics Evaluation in Enugu Urban, Nigeria

Chinyere Salome Ofordu, Chukwuka Friday Agbor*, Oseyomon John Aigbokhan, Monsurah Abiola Audu, Ekundayo David Adedoyin, Obianuju Maureen Ogoliegbune

Environmental Modeling and Biometrics, Forestry Research Institute of Nigeria, Jericho, Ibadan, Nigeria
Email: *chukwuka_friday@yahoo.com

How to cite this paper: Ofordu, C. S., Agbor, C. F., Aigbokhan, O. J., Audu, M. A., Adedoyin, E. D., & Ogoliegbune, O. M. (2022). Urban Heat Island and Land Use/Cover Dynamics Evaluation in Enugu Urban, Nigeria. *Journal of Geoscience and Environment Protection, 10,* 354-372.
https://doi.org/10.4236/gep.2022.1012020

Received: July 23, 2022
Accepted: December 27, 2022
Published: December 30, 2022

Abstract

This study specifically estimated the effect of land use/cover change (LULC) processes on land surface temperature (LST) in Enugu urban and its suburbs. With Landsat images and supervised classification technique, four LULC classes comprising built-up areas, vegetation, rock outcrop, bare ground/farmland areas were delineated. The LST was extracted from the thermal bands of the images. The rate of change in land cover classes between 2009 and 2018 showed that from 2009 to 2013, built-up areas increased from 31.65% to about 47.5%, while vegetation cover decreased from 18.43% to 11.23%. Also, the periods witnessed about 8.69 km^2 of vegetation being converted to other land surfaces. The trend in the LST in Enugu urban showed the highest mean temperatures of 34.5˚C in 2018 and 32.26˚C in 2015. However, in 2013 there was a slight decrease in mean LST to 31.65˚C which further decreased to 31.26˚C in 2009. This change in temperature suggests that urbanisation could have significant effect on the micro-climate of Enugu city. Result also revealed weak relationships between LULC classes and the LST throughout the years. The results of the surface heat intensity for the urban and rural areas showed general increase over the years and this suggests that rural areas are also experiencing high temperature which could be due to the loss of vegetation, increase in artificial surfaces and urban encroachment. Findings from this study could be useful for effective urban land-use planning, policy development and management in Nigeria, and elsewhere.

Keywords

Land Use/Cover Change, Land Surface Temperature, Urbanisation, Micro-Climate, Surface Heat Intensity

1. Introduction

Surface modifications due to urbanization generally lead to a modified thermal climate that is warmer than the surrounding rural area (EPA, 2009). This phenomenon is known as the urban heat island (UHI). A combination of factors such as building materials, thermal properties, urban design geometry or urban canyons, anthropogenic factors, built environment result in the development of UHI (EPA, 2009). UHI intensity is reported to be stronger at night time and increases when the size of the city increases (Wang et al., 2015a). UHI effects vary seasonally, and it is more apparent during the dry season (Awuh & Amawa, 2017; Aslan & Koc-San, 2016; Alhawiti & Mitsova, 2016; Enete et al., 2014). Anthropogenic factors such as waste, heat of vehicles and buildings alter land surface cover in a way that porous surfaces are replaced with non-porous materials, thus restricting evaporation and cooling of the city (Wang et al., 2015a).

Urban Heat Island studies are important to urban climatologists, urban planners and the health sectors and more important for the comfort of urban residents and can be studied by means of Land Surface Temperature (LST) and air temperature difference between urban and rural areas (Wang et al., 2015b). Previous studies have demonstrated that the LST product retrieved from thermal infrared (TIR) sensors can be used to monitor the UHI effect (Lin et al., 2005; Weng & Fu, 2014). Land Surface Temperature (LST) provides an accurate measure for indicating energy exchange balance between the Earth and the atmosphere (Liu & Zhang, 2011). Land surface temperature which is controlled by the surface energy balance, atmospheric state and thermal properties of the surface and subsurface rocks, is one of the important parameters in several environmental models in studying UHI (Becker & Li, 1990). Land surface temperature is important for environmental studies and management of the Earth's resources because it determines the effective radiating temperature of the Earth's surface. Also, it is a major factor in determining the partition of the available energy into sensible and latent heat fluxes (Fabrizi et al., 2010).

The advent of thermal remote sensing technology has made observation of UHI possible using Satellite and Aircraft platforms (Chen et al., 2017; Kurnia et al., 2016). This has provided new path for the study of UHI and their effects through the combination of thermal remote sensing and urban micrometeorology (Voogt & Oke, 2004). A number of satellite methods are available that can be used to examine the LST and determine the UHI effects. Landsat Bands are the data that are most widely used for these studies (Jiménez-Muñozoz et al., 2014; Jin et al., 2015; Sekertekin et al., 2016; Wang et al., 2015b; Yu et al., 2014). Several studies (Wang et al., 2015a; Allegrini et al., 2015; Tyubee & Anyadike, 2015; Usman, 2013; Qin et al., 2001; Awuh et al., 2018; Awuh et al., 2019) have estimated air temperatures using Landsat TM Imageries.

Urban Heat island studies is well-documented in Enugu (Enete & Alabi, 2012; Enete & Okwu, 2013), the effect of land use change on UHI (LST) has not been previously studied. Therefore, this work determined the degree of LULCC and

the impact on UHI in Enugu Urban using Landsat imageries.

2. Method and Materials

2.1. Study Area

Enugu is a south-eastern State in Nigeria, which lies at approximately longitudes 6˚ and 14˚E and latitudes 7˚ and 10˚N as shown in **Figure 1**. It is has an estimated population of 4,427,766 and approximately 77,310 km^2, with about 9.82% (423,272) of the total population located in the urban areas (Ofordu et al., 2019). Enugu has a tropical climate with two distinct seasons, a dry period from November to April, and a rainy season April to October. Although, the heaviest rains (up to 360 mm) occur between June and July, while the lowest rainfall level (up to 16 mm) occur in February. The mean annual temperature range is usually between 26.8˚C and 32.5˚C. The predominant land uses in Enugu City are residential, commercial, industrial and institutional. Most of the residential areas in the City were planned and built according to the grid-iron pattern. Apart from

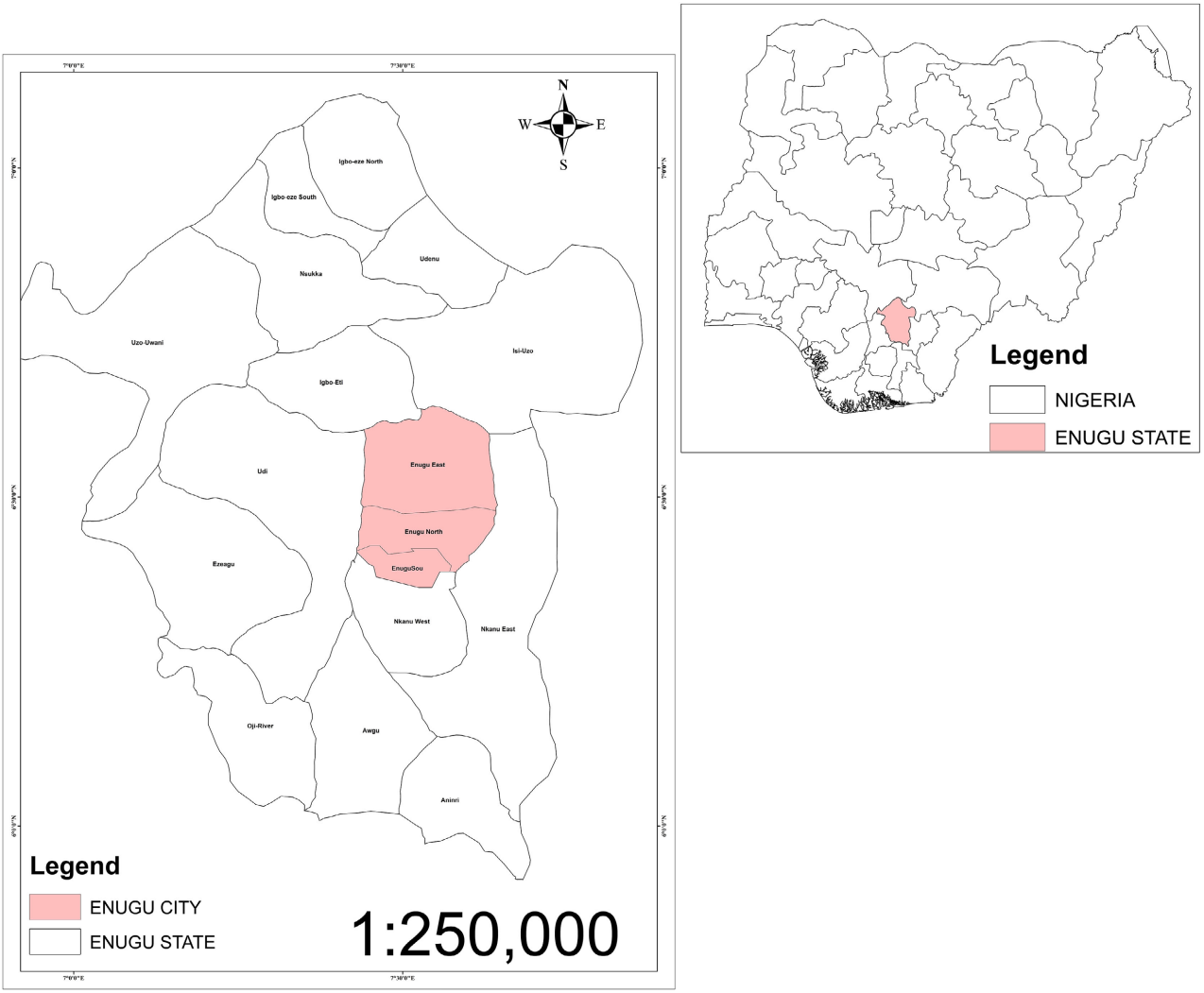

Figure 1. Enugu urban area (Source: Ofordu et al., 2019).

the markets in Enugu urban, most of the poor households locate their commercial activities virtually along all road corners using residential buildings for commercial uses, bringing about mixed land use. Mixed land use is a major characteristic in most Nigerian cities (Awuh et al., 2018). It is one of the coping strategies used by poor households in Enugu urban area.

2.2. Data Collection

Primary data were obtained using the Mono Window Algorithm Technique. Landsatimages i.e. the Thematic Mapper (TM) for 2009, Metadata Enhanced Thematic Mapper Plus (ETM+) for 2012 and Operational Land Imagery (OLI) for 2018 were downloaded from the United States Geologic Survey (USGS) archive for the period 2009 to 2018 at three (3) years interval. The use of 3 years interval was to allow for uniformity between the datasets. The satellite data has 30 m spatial resolutions, with the TM and ETM+ having a spectral range of 0.45 - 2.35 micrometer (μm) in Bands 1 to 7 and 8 respectively, while the Operational Land Imagery (OLI) extended to Band 11. The shapefile delineating the boundary of the study area were obtained from the National Space Research and Development Agency (NASRDA). Additionally, secondary data were obtained from the Nigeria Meteorological Agency.

2.3. Image Classification for LULC Extractin

All the images were pre-processed by the USGS to rectify any geometric or radiometric distortions of the image. This correction process employed both Digital Elevation Models and Ground Control Points to achieve a product that was free from distortions related to the Earth (e.g. curvature, rotation), satellite (e.g. attitude deviations from nominal), and sensor (e.g. view angle effects). The USGS also geometrically corrected and georeferenced both images to the WGS1984 datum and Universal Transverse Mercator (UTM) zone 32N coordinate system. A supervised classification scheme with the Interactive Selection algorithm was used for the classification (Yang et al., 2017). The supervised classification was performed by creating a training sample, and based on spectral signature curve, various land uses were extracted (Agbor et al., 2012).

2.4. Retrieval of Land Surface Temperature

The Landsat 5 and 7 thermal bands 6 and TIRS 10 were considered suitable as shown by many literatures for capturing the multifaceted intra-urban temperature differences thus making it effective for urban climate analysis. Consequently, the Landsat thermal bands were used to retrieve LST of the study area (Agbor & Makinde, 2018) for the four different periods (2009, 2013, 2015 and 2018) using various procedures which range from radiometric calibration, conversion of DN to radiance, correction for atmospheric absorption, re-emission and surface emissivity (Awuh et al., 2018; Makinde & Agbor, 2019) as described below:

Conversion of Digital Numbers (DN) of the bands to Spectral Radiance

$$L_{\lambda} = \left[\frac{L_{MAX} - L_{MIN}}{Q_{Calmax} - Q_{CALMIN}} \right] \times (DN - 1) + L_{MIN} \quad (1)$$

where,

L_{MAX} = the spectral radiance that is scaled to Q_{CALMAX} in W/(m² * sr * μm) L_{MIN} = the spectral radiance that is scaled to Q_{CALMIN} in W/(m² * sr * μm) Q_{CALMAX} = the maximum quantized calibrated pixel value (corresponding to L_{MAX}) in DN = 255 Q_{CALMIN} = the minimum quantized calibrated pixel value (corresponding to L_{MIN}) in DN = 1.

Conversion from Spectral Radiance to At-Satellite Brightness Temperature

$$T = \frac{K_2}{\ln\left(\frac{K_1}{L_{\lambda}} + 1\right)} - 273.15 \quad (2)$$

where, T = At-satellite brightness temperature, L_l = Spectral radiance (gotten from Equations (1), K_1 = Band specific thermal conversion constant from the metadata, K_2 = Band specific thermal conversion constant from the metadata, −273.15 = Constant for conversion from Kelvin to Degrees Celsius as shown in Awuh et al. (2018). The temperature values obtained using Equation (2) are reference to a blackbody. Therefore, corrections for spectral emissivity (ε) became necessary according to the nature of land cover:

$$e = 0.004 P_V + 0.986 \quad (3)$$

where, e = Land Surface Emissivity, 0.004 & 0.986 = Constants for emissivity estimation, P_V = Proportion of vegetation (Awuh et al., 2018) given by the equation

$$P_V \left(\frac{NDVI - NDVI_{min}}{NDVI_{max} - NDVI_{min}} \right) \quad (4)$$

And

$$NDVI = \frac{\rho NIR - \rho Red}{\rho NIR + \rho Red} \quad (5)$$

where

ρNIR = near-infrared reflectance;

ρRed = red reflectance.

The Normalized Differential Vegetation Index was computed with Equation (5) for each of the years, $NDVI_{min}$ = Minimum value of NDVI for that year, $NDVI_{max}$ = Maximum value of NDVI for that year (Awuh et al., 2018).

Estimation of the Land Surface Temperature

$$LST = \frac{B_T}{1 + W} \times \frac{B_T}{P} \times \ln(\Sigma) \quad (6)$$

where, LST= Land Surface Temperature, B_T = At-satellite brightness temperature, W= Wavelength of emitted radiance (μm) Awuh et al. (2018) given as:

$$P = h \times \frac{c}{s} \left(1.438 \times 10^{-2}\ \text{m} \cdot \text{K}\right) = 14380 \quad (7)$$

h = Planck's constant (6.626×10^{-34}/s),

S = Boltzmann constant 1.38×10^{-23} j/k), C = Velocity of light (2.998×10^{8} m/s), e = LSE.

Pearson's Product Moment Correlation analyses were carried out to determine the relationship between land use and land covers and land surface temperature. The Pearson's Product Moment Correlation Analysis is a statistical method that tests the measures of linear association between two quantitative variables, with the linear association going from +1 to −1 in decreasing order of strength. This equation is given as:

$$r = \frac{\sum XY - \frac{(\sum X)(\sum Y)}{N}}{\left(\sum X^2 - \frac{(\sum X)^2}{N}\right)\left(\sum Y^2 - \frac{(\sum Y)^2}{N}\right)} \tag{8}$$

where r = Correlation Coefficient

X = Independent variable, which is the Land use classes in decreasing order of reflective capacity;

Y = Dependent variable, which is the land surface temperature readings associated with each class;

n = Observations.

To test the strength of the correlation, the coefficient of determination was used and given by:

$$C/D = r^2 \tag{9}$$

where C/D = Coefficient of determination;

r^2 = Coefficient of determination.

To determine the relationship between the land use land cover classes and the Land Surface Temperature between 2009 and 2018, a subpixel correlation and regression analysis was performed (Makinde & Agbor, 2019). Since linear relationships are either positive or negative, the intercept will be the value for the dependent variable when each of the independent variables takes on a value of zero. The correlation coefficient (r) indicates the effects of the independent variables on the dependent variable. The R square (R^2) or adjusted R square represents the extent of variability in the dependent variable explained by the independent variables. In this study, the independent and dependent variables respectively, represents or explains the causes and the effects of an action (Ahmed et al., 2013).

2.5. Research Hypothesis Testing

A statistical hypothesis test is a method of statistical inference used to determine a possible conclusion from two different and likely conflicting hypotheses (Raymond & Bayarri, 2013). The following hypotheses were tested:

1) There is no significant change in the annual temperature trend in Enugu Urban in the past 9 years (2009-2018).

2) There is no significant relationship between land-use and land-cover change and urban heat island in the Enugu Urban.

3. Results

3.1. Land Use Land Cover Changes between 2009 and 2018

From Table 1, we observed 47.5% of the total land area was predominately occupied by built-up areas. This was followed by areas classified as bare ground or farmland in about 36% of the spatial coverage. In addition, the vegetation and rock outcrop classes occupied 17% of the total land area. The Area coverage of the classes shows the extent of change of the different classes for the period 2009 to 2018. For example, it was observed that built-up areas had changed significantly within the last three year period of 2013 to 2018. About 63.8% of other land cover types were lost to urbanization between 2015 to 2018 in contrast to the 3.1% of urban areas to other land surfaces.

The rate of change that occurred within the land cover classes for the period of 2009 to 2018 are presented in Table 2. The result showed that between 2009 and 2013, built-up areas increased with about 12.43% whereas a notable loss (8%) of land area previously occupied by vegetation was observed. The conversion and loss of vegetation is probably due to the conversion to other land uses in the urban area. Also, due to urban development and other factors, between 2009 and 2013 about 5.7% of land area previously classified as rocky areas have been converted to other surfaces, mostly residential and/or commercial areas, for example, the Coal Camp areas in Enugu urban. However, being that the Landsat Imagery was captured during the dry season, a lot of the areas that would have

Table 1. Distribution of land use land cover classes for 2009 to 2018.

Classes	2009 (Km^2)	(%)	2013 (Km^2)	(%)	2015 (Km^2)	(%)	2018 (Km^2)	Total (%)
Built-up	55.15	31.65	76.80	44.08	78.55	45.08	120.56	47.50
Vegetation	32.11	18.43	18.14	10.41	11.19	6.42	16.83	11.23
Rock outcrop	23.41	13.44	13.51	7.75	1.91	1.10	0.96	5.71
Bare ground/Farmland	63.561	36.48	65.79	37.76	82.60	47.40	35.89	35.56
Total area	174.24	100	174.24	100	174.24	100	174.24	100

Source: Researchers' GIS Lab (2019).

Table 2. Percentage changes of land use land cover classes for 2009 to 2018.

Classes	2009-2013 (%)	2013-2015 (%)	2015-2018 (%)
Built-up	12.43	1	2.42
Vegetation	−8.02	−3.99	4.81
Rock outcrop	−5.69	−6.65	4.61
Bare ground and/or Farmland	1.28	9.64	11.84

Source: Researchers' GIS Lab (2019).

been cultivated during the rainy seasons were now left bare and they occupy a total of 1.3% of the total landmass between 2009 and 2013.

We can also deduce from Table 2 above that between 2013 to 2015 notable changes occurred in each of the classes. Although built-up areas increased slightly at the rate of 1% when compared to previous year, it was observed that about 6.65% of the rocky areas were encroached and converted for urban development whereas vegetated areas decreased at the rate of 3.99%. Also, the bare ground or farmland areas increased with about 9.64% mostly due to land clearing and harvested plots of land.

Moreover, the periods 2015 to 2018 witnessed 2.42% increase in areas being converted to artificial surfaces. This increase in built-up areas could have occurred mostly from rural-urban migration or other urban development that will require more land areas for housing, infrastructure, or other needs to accommodate the increasing population. It was however observed that vegetation cover which had been on the decrease since 2009 suddenly increased by 4.81% in 2018 This trend could be due to the increasing awareness of people living in cities on the need for tree planting and/or the negative impacts of climate change on humans and the environment. Of a sad note, however, the rocky areas are continuously converted to other land uses. The results represented in the Landsat imageries in Figures 2(a)-(d).

3.2. Distribution of Temperature within the Study Area

As shown in Figure 3(a)-(d), the Landsat Imageries depicts the spatio temporal trend of the Mean Land Surface Temperature (MLST) in Enugu urban. It showed the highest urban mean temperature of 34.5˚C was recorded in 2018, followed by 2015 with a mean temperature of 32.26˚C. However, in 2013 and 2015 there was a slight increase in temperature to about 0.4˚C as shown in Table 3. Mean temperature was lower in the rural area than in the city with slight difference in temperature changes over the years (Table 4). The change in temperature

Table 3. Mean land surface temperature in urban areas.

Year	High (˚C)	Changes (˚C)
2009	31.26	-
2013	31.65	0.4
2015	32.26	0.61
2018	34.5	2.24

Table 4. Mean land surface temperature in rural areas.

Year	High (˚C)	Change (˚C)
2009	25.76	-
2013	29.36	3.6
2015	29.75	0.39
2018	32.16	2.41

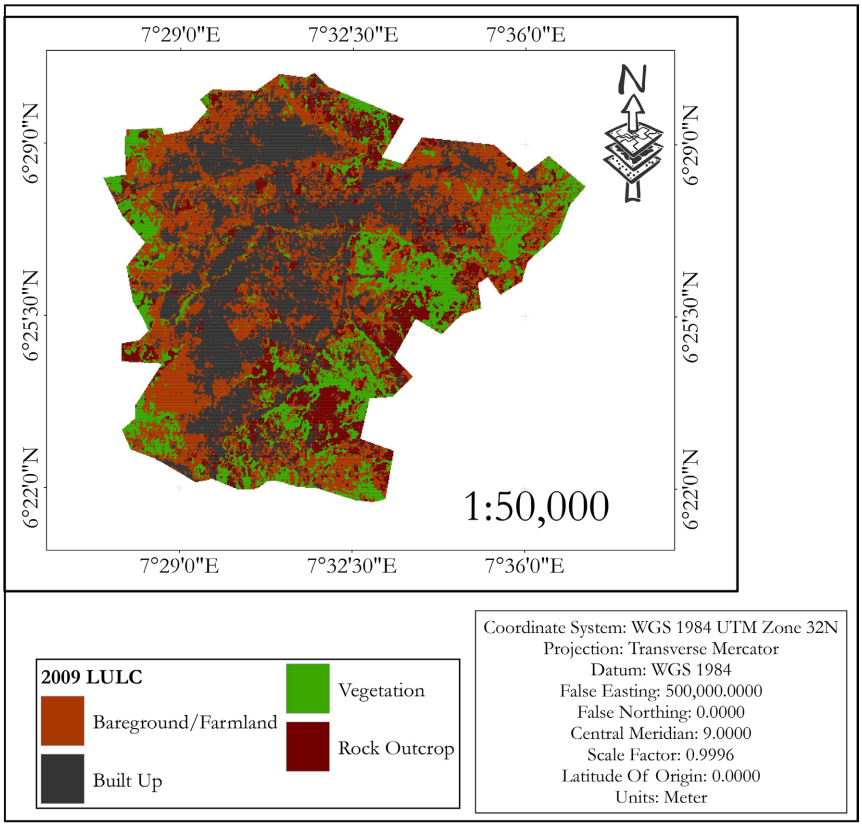
7°29'0"E
7°32'30"E
7°36'0"E
6°29'0"N
6°25'30"N
6°22'0"N
N
1:50,000
2009 LULC
Bareground/Farmland
Built Up
Vegetation
Rock Outcrop
Coordinate System: WGS 1984 UTM Zone 32N
Projection: Transverse Mercator
Datum: WGS 1984
False Easting: 500,000.0000
False Northing: 0.0000
Central Meridian: 9.0000
Scale Factor: 0.9996
Latitude Of Origin: 0.0000
Units: Meter

(a)

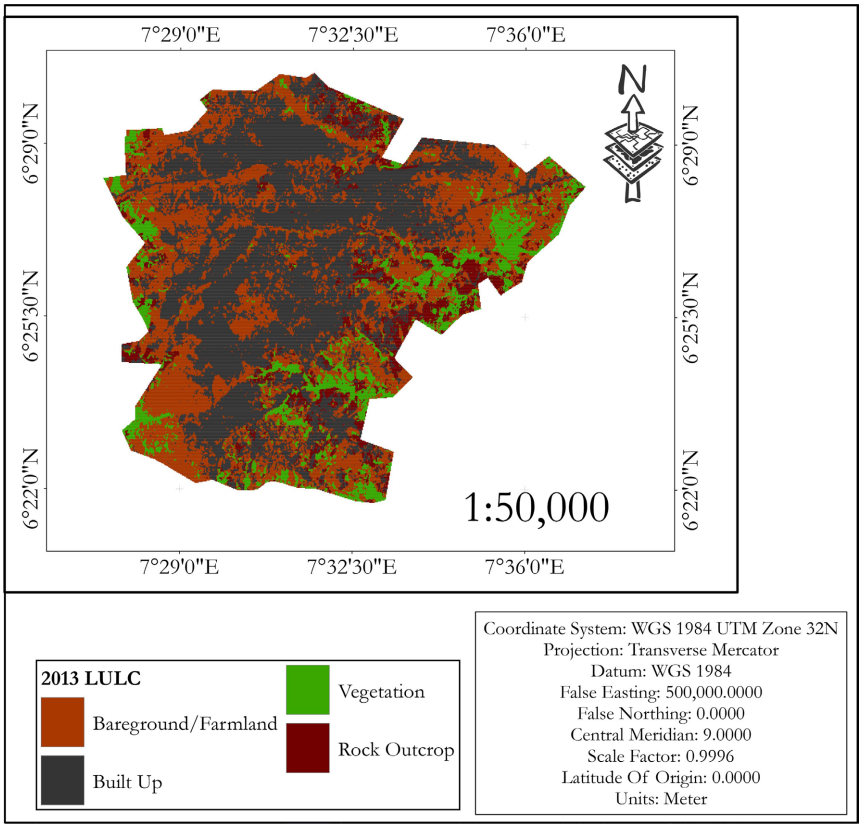
7°29'0"E
7°32'30"E
7°36'0"E
6°29'0"N
6°25'30"N
6°22'0"N
N
1:50,000
2013 LULC
Bareground/Farmland
Built Up
Vegetation
Rock Outcrop
Coordinate System: WGS 1984 UTM Zone 32N
Projection: Transverse Mercator
Datum: WGS 1984
False Easting: 500,000.0000
False Northing: 0.0000
Central Meridian: 9.0000
Scale Factor: 0.9996
Latitude Of Origin: 0.0000
Units: Meter

(b)

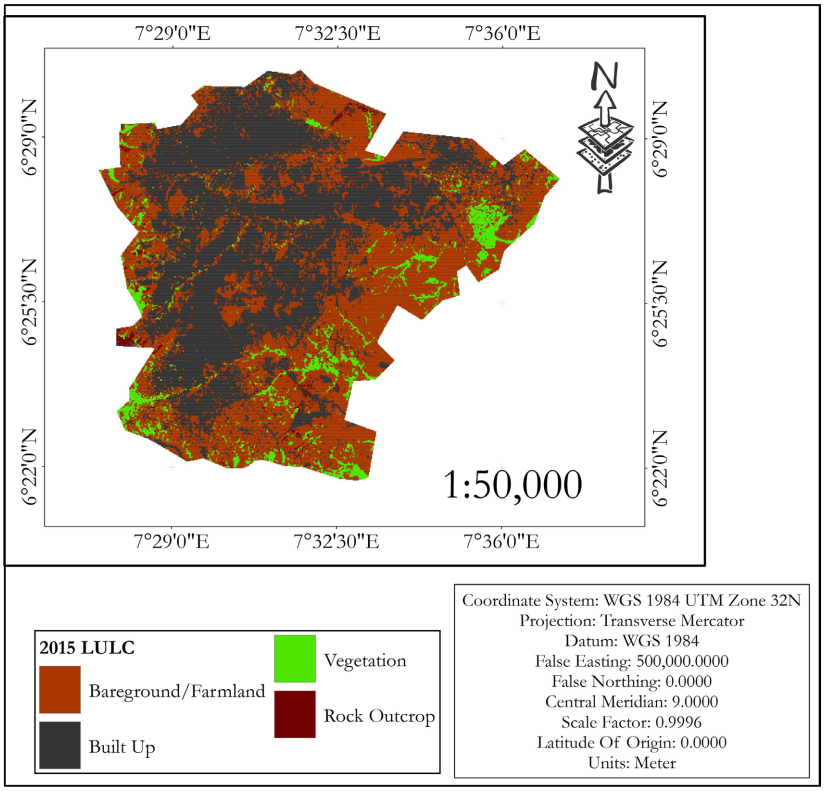

(c)

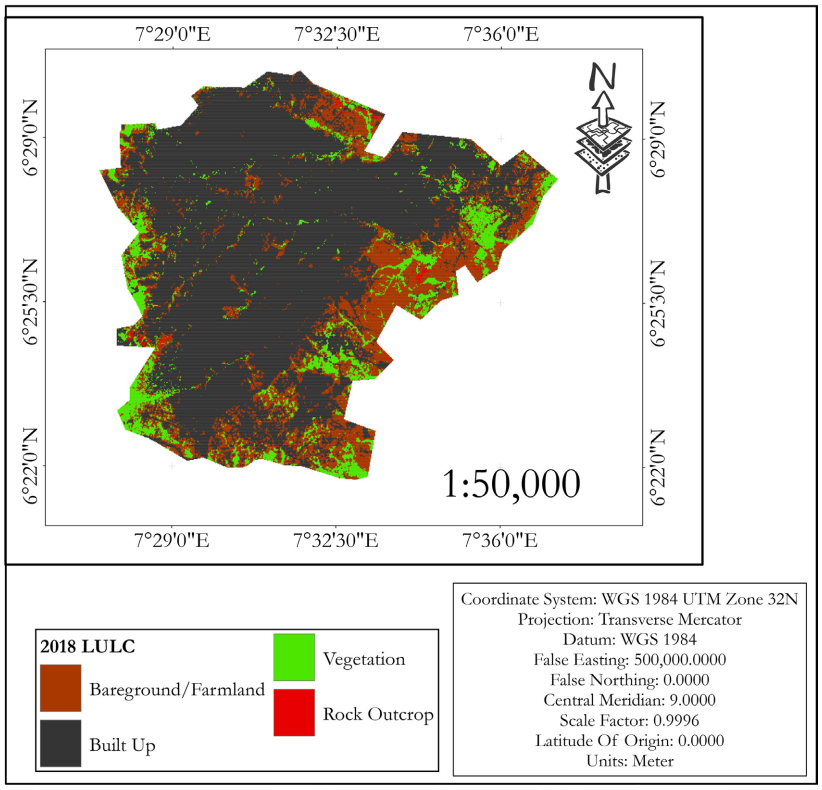

(d)

Figure 2. (a, b) Changes in different land use classes in (a) 2009 and (b) 2013; (c, d) Changes in different land use classes in (c) 2015 and (d) 2018.

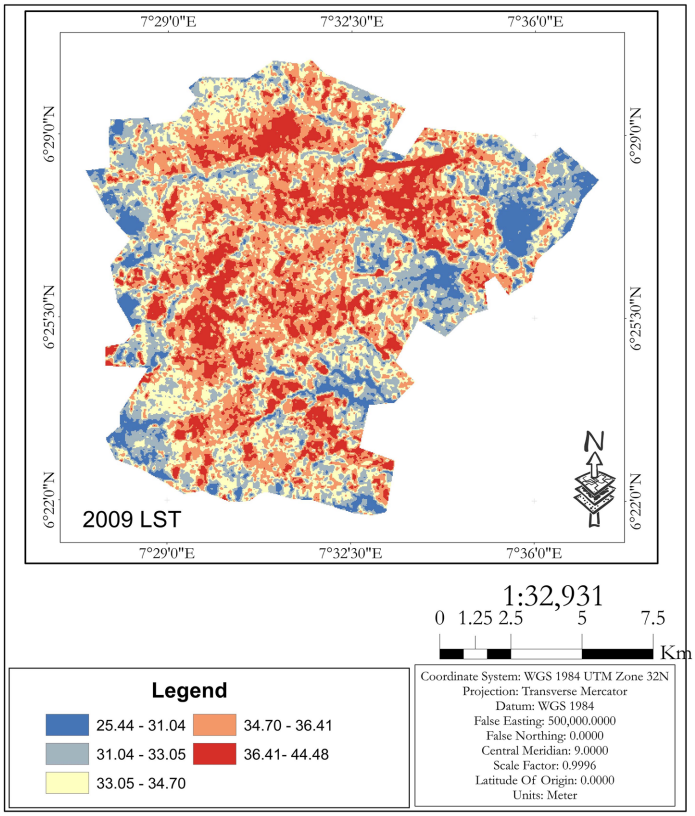
7°29'0"E
7°32'30"E
7°36'0"E
6°29'0"N
6°25'30"N
6°22'0"N
2009 LST
N
1:32,931
0 1.25 2.5 5 7.5
Km
Legend
25.44 - 31.04
34.70 - 36.41
31.04 - 33.05
36.41- 44.48
33.05 - 34.70
Coordinate System: WGS 1984 UTM Zone 32N
Projection: Transverse Mercator
Datum: WGS 1984
False Easting: 500,000.0000
False Northing: 0.0000
Central Meridian: 9.0000
Scale Factor: 0.9996
Latitude Of Origin: 0.0000
Units: Meter

(a)

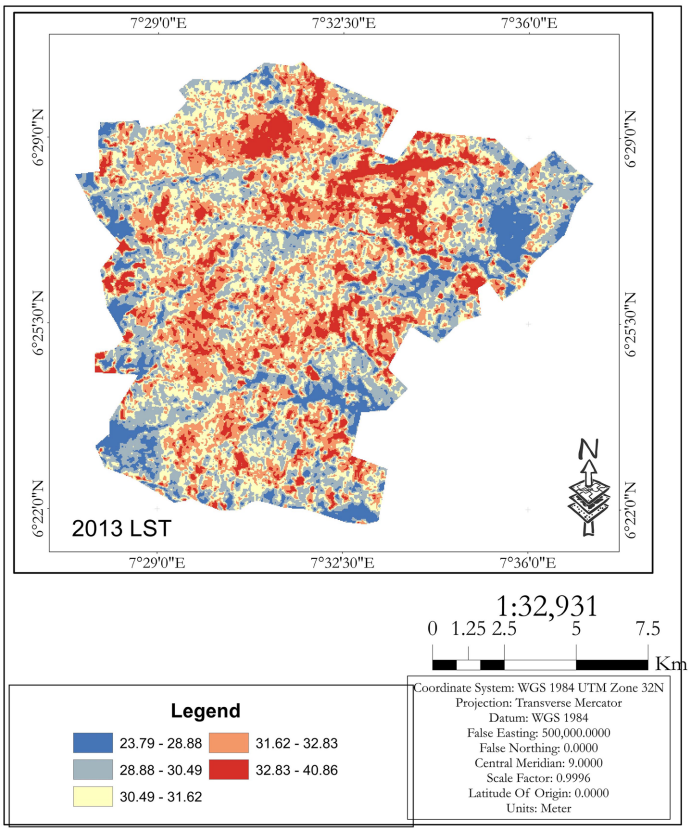
7°29'0"E
7°32'30"E
7°36'0"E
6°29'0"N
6°25'30"N
6°22'0"N
2013 LST
N
1:32,931
0 1.25 2.5 5 7.5
Km
Legend
23.79 - 28.88
31.62 - 32.83
28.88 - 30.49
32.83 - 40.86
30.49 - 31.62
Coordinate System: WGS 1984 UTM Zone 32N
Projection: Transverse Mercator
Datum: WGS 1984
False Easting: 500,000.0000
False Northing: 0.0000
Central Meridian: 9.0000
Scale Factor: 0.9996
Latitude Of Origin: 0.0000
Units: Meter

(b)

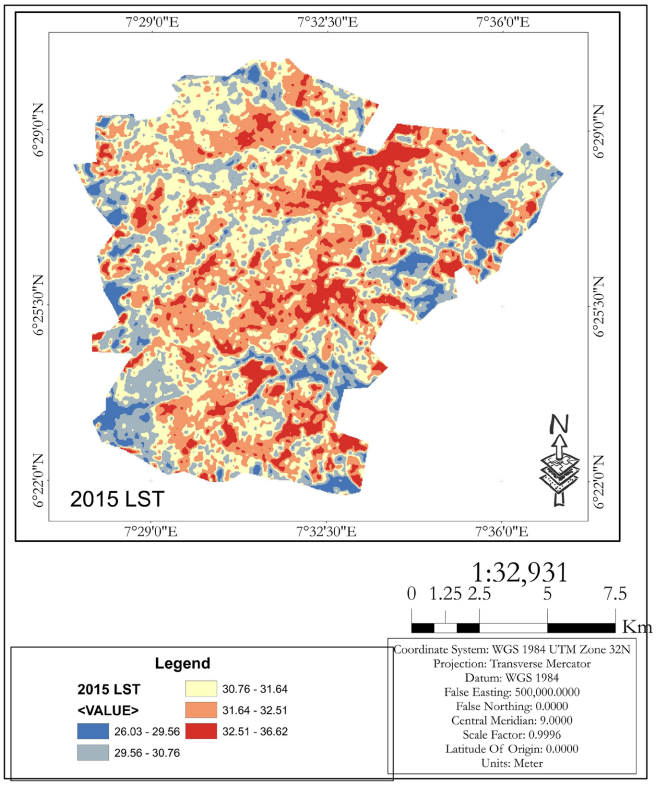

(c)

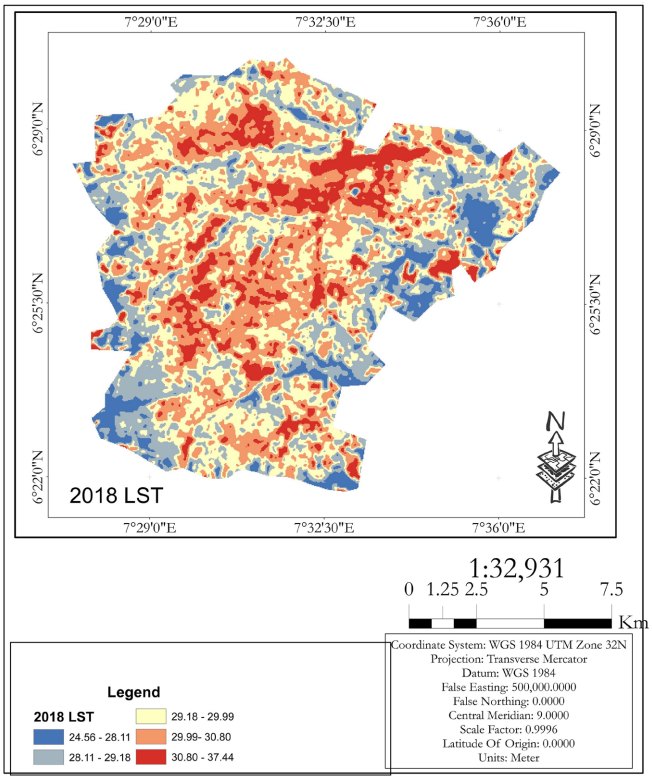

(d)

Figure 3. (a, b) Land surface temperature of Enugu urban in 2009 and 2013; (c, d) Land surface temperature of Enugu urban in 2015 and 2018.

suggests that urbanisation could have significant effect on the micro-climate of Enugu city. Also, the variations in temperature could be attributed to increasing artificial surfaces and loss of vegetation cover in both rural and urban areas.

Furthermore, from Table 5, it was noted that most of the natural open spaces formerly occupied by rock outcrop, bare ground or farmland and vegetation have been converted to built-up and artificial surfaces. This has greatly affected the micro-climate of the area.

3.3. The Urban Heat Intensity (SUHI)

The high Surface Urban Heat Intensity (SUHI) that we selected was derived from the highest temperature from our control points in the urban areas and then subtracted from the highest temperature obtained from the rural areas (see Table 6). It was observed that the lowest variation of 0.5˚C was recorded in 2009 while the highest variation of 2.37˚C was observed in 2018.

In order to derive the lowest Surface Urban Heat Intensity (SUHI), the lowest

Table 5. Changes in the different land use classes.

S/N	Name	AREA
1	**Built Up to Built-Up**	**27.51**
2	Built Up to Vegetation	1.16
3	Built Up to Rock Outcrop	1.83
4	Built Up to Bare ground or Farmland	2.42
5	**Vegetation to Built-Up**	**0.81**
6	Vegetation to Vegetation	0.02
7	Vegetation to Rock Outcrop	4.86
8	Vegetation to Bare ground or Farmland	3.01
9	**Rock Outcrop to Built-Up**	**57.09**
10	Rock Outcrop to Vegetation	0.23
11	Rock Outcrop to Rock Outcrop	6.49
12	Rock Outcrop to Bare ground or Farmland	15.41
13	**Bare ground or Farmland to Built-Up**	**53.19**
14	Bare ground or Farmland to Vegetation	0.08
15	Bare ground or Farmland to Rock Outcrop	0.12

Table 6. High surface heat intensity.

Year	Urban (˚C)	Rural (˚C)	Change (˚C)
2009	31.26	30.76	0.5
2013	33.65	32.36	1.29
2015	34.26	33.75	0.51
2018	38.53	36.16	2.37

temperature range from our control points were selected and analysed. The variations were observed to be higher than what was gotten from the High SUHI (see Table 7).

In this study, 4.98˚C, 3.61˚C, 2.38˚C and 3.07˚C were recorded for 2009, 2013, 2015 and 2018 respectively. It was observed that 2013 had the highest variation (3.53˚C) while the lowest (2.38˚C) was recorded in 2015. These variations suggests that rural areas are also experiencing high temperature which could be due to the loss of vegetation, increase in artificial surfaces, urban encroachment, loss of natural bodies such as rivers or streams, amongst others

3.4. Validation of Derived LST Using Ground Recorded Temperature

In this study, the derived mean Land Surface Temperature (LST) data which was gotten from satellite imagery was validated with the ground recorded mean temperature that was gotten from NIMET for the same years and month. As observed in Table 8 the difference between the derived and recorded temperature for 2018 was −0.7˚C. Also, the highest difference between the two sources was noted in 2009 where we had a variation of 3.34˚C. We can deduce that the LST from the satellite imagery could serve as a good substitute in analysing the temperature of an area at any given time.

3.5. The LULC and LST Relationship

The result of the linear regression showed that in 2009 there was a weak positive relationship ($r = 0.195$) between the different land use land cover classes and the surface temperature. The coefficient of determination (r^2) value of 0.52 indicated that 52% of the variability in land surface temperature in 2009 can be explained by the different land use land cover classes of that year (Table 9). However, in 2018 the result of the linear regression revealed a negative relationship ($r = -0.183$) between the different land use land cover classes and the surface temperature. The coefficient of determination (r^2) value of 0.335 indicated that only 33.5% of the variability in land surface temperature in 2018 can be explained by the different land use land cover classes of that year. Therefore, it can be inferred that the relationship between the LULC classes and LST dynamics was significant in year 2018 as compared to 2009 because the higher the coefficient of determination, the stronger the relationship between the independent and dependent variables, as observed in the year 2018.

3.6. Tests of Hypotheses

The results of the tests for the various hypotheses are presented in Table 10.

For hypothesis i, with mean annual temperature of 34.43, the calculated t-value is 308.750, which is greater than the critical t-value of 1.833. This indicates that there is a difference in annual temperatures for the study period from 2009 to 2018. With a p-value of $0.000 < 0.05$, this difference is significant. Based on this, the null hypothesis is rejected.

Table 7. Low surface urban heat intensity.

Year	Urban (˚C)	Rural (˚C)	Change (˚C)
2009	29.4	26.25	3.15
2013	29.86	26.33	3.53
2015	30.45	28.07	2.38
2018	32.85	27.87	3.07

Table 8. Validation of the derived land surface temperature using ground recorded temperature.

Year	Source of temperature data		
	NIMET (˚C)	Mean LST from satellite imagery (˚C)	Difference (˚C)
2009	34.6	31.26	3.34
2013	32.6	31.65	0.95
2015	32.7	32.26	0.44
2018	33.8	34.5	−0.7

Table 9. LULC and LST relationships in 2009 and 2018.

Year	Equations	r^2	r
2009	$y = 20.73 + 0.195x$	0.52	0.072
2018	$y = 21.35 - 0.232x$	0.35	−0.18

Table 10. Hypothesis tests between 2009 and 2018.

Hypotheses	T-Test Result			
	T-test calculated value	P-value	r	r^2
i	308.75	0.000	-	-
ii	-	$P < 0.05$	−0.183	0.335

The result of hypothesis ii reveals that there is a negative relationship between land use land cover and the surface temperature ($r = -0.183$). The coefficient of determination (r^2) shows that 33.5% of the variability in land surface temperature can be explained by the different landuse and landcover classes. Since $p < 0.05$, this result is significant, therefore, the null hypothesis is rejected. Hence, there is significant relationship between land use and land cover change and urban heat island in Enugu urban.

4. Discussion of Findings

The findings from this study revealed significant difference in annual temperature over the years and substantial impact of LULC on LST. Between 2009 and 2013, there was a steady increase in built-up areas with about 12.43% and a sig-

nificant loss of vegetation areas to about 8.02%. This corroborates Turner et al. (2007) report that due to rapid urbanization land previously classified as rocky areas have been converted to industrial, residential and other uses. It was observed that land use and land cover classes were not static but experienced continuous change. This alteration is referred to as a modification of the earth terrestrial surface (Turner et al., 2007). Also, rural-urban migration could have triggered the construction of more housing layouts to accommodate population surge thereby increasing the urban heat emission. As shown in **Table 5**, temperature has continued to increase, suggesting that increasing influx of migrants or rapid urbanization could trigger the increase in temperature in Enugu urban. This is because heat stored in structures is released to the environment when the sun sets (Oke, 1987). Also, more structures could mean greater heat emission. The findings revealed temperature increased at the urban centers and the suburbs. Our research also showed that Enugu urban was experiencing general loss in it's natural land cover such as vegetation, rock outcrops, bare grounds and cultivated lands. This could be attributed to urbanization which may be as a result of the influx of population into the city (Makinde & Agbor, 2019). The presence of natural land covers such as vegetation and water bodies play a significant role in lowering the temperature of a place whereas the absence of such triggers hotter conditions as can be seen in Enugu City (Mango, 2010). Most thick vegetated areas are found on rock outcrops with the ability to aid orographic rainfall formation. But, if we continue to lose them, it will negatively impact on the climate of urban areas like Enugu. This suggests that the importance of the rock outcrop if underrated or undermined could affect their impact in climate regulation in urban areas.

5. Conclusion

This study will act as a catalyst in rekindling an already existing research in urban climatology in Nigeria especially in higher institutions of learning and research. Knowledge of land use change occurrence and the impacts are important in environmental management. It analyzed the spatio-temporal changes that occurred within the Land use types and the different natural Landcover that exists within Enugu city over the years 2009-2018. We also studied the trends of the Urban Heat Island which was derived from the thermal bands of Landsat images using the Land Surface Temperature methodology. The relationship that existed between Land Surface Temperature (LST) and Land use Land cover classes was reported. The Surface Urban Heat Intensity was calculated and the temperature differences between the urban and rural areas were further determined. In other to validate the derived LST, temperature data records from weather stations within the city for the same month and years were gotten from Nigerian Meteorological Agency (NIMET) and the two data were compared. The findings revealed temperature increased at the urban centers and the suburbs. Our research also showed that Enugu urban was experiencing general loss

in her natural land cover such as vegetation, rock outcrops, bare grounds and cultivated lands. This could be attributed to urbanization which may be as a result of the influx of population into the city.

The urban fringes consisting of the suburbs and the rural areas which ought to act as a natural buffer in regulation of urban temperature also recorded high temperature ranges and this could pose a great threat to the environment. The high temperatures which were recorded in the study area could be attributed to increased urban population, urban encroachment into the fringes, amongst others.

Conflicts of Interest

The authors declare no conflicts of interest regarding the publication of this paper.

References

Agbor, C. F., & Makinde, E. O. (2018). Land Surface Temperature Mapping Using Geoinformation Techniques. *Geoinformatics FCE CTU, 17,* 17-32. https://doi.org/10.14311/gi.17.1.2

Agbor, C. F., Aigbokhan, O. J., Osudiala, C. S., & Malizu, L. (2012). Land Use Land Cover Change Prediction of Ibadan Metropolis. *Journal of Forestry Research and Management, 9,* 1-13.

Ahmed, B., Kamruzzaman, Zhu, X., Rahman, S., & Choi, K. (2013). Simulating Land Cover Changes and their Impacts on Land Surface Temperature in Dhaka, Bangladesh. *Remote Sensing, 5,* 5969-5998. https://doi.org/10.3390/rs5115969

Alhawiti, B. H., & Mitsova, D. (2016). Using Landsat-8 Data to Explore the Correlation between Urban Heat Island and Urban Land Uses. *International Journal of Research in Engineering and Technology, 5,* 457-466. https://doi.org/10.15623/ijret.2016.0503083

Allegrini, J., Dorer, V., & Carmeliet, J. (2015). Influence of Morphologies on the Microclimate in Urban Neighbourhoods. *Journal of Wind Engineering and Industrial Aerodynamics, 144,* 108-117. https://doi.org/10.1016/j.jweia.2015.03.024

Aslan, N., & Koc-San, D. (2016). Analysis of Relationship between Urban Heat Island Effects & Land Use/Land Cover Type Using Landsat 7 ETM+ and Landsat 8 OLI Images. *International Archives of the Photogrammetric, Remote Sensing and Spatial Information Sciences, XLI-B8,* 821-828. https://doi.org/10.5194/isprsarchives-XLI-B8-821-2016

Awuh, M. E., & Amawa, S. G. (2017). Urban Heat Island Coping/Adaptive Strategies in Douala Metropolis Cameroon. *Journal of Geography Meteorology and Environment Studies, 4,* 329-347.

Awuh, M. E., Japhets, P. O., Officha, M. C., Okolie A. O., & Enete, I. C. (2019). A Correlation Analysis of the Relationship between Land Use and Land Cover/Land Surface Temperature in Abuja Municipal, FCT, Nigeria. *Journal of Geographic Information System, 11,* 44-55. https://doi.org/10.4236/jgis.2019.111004

Awuh, M. E., Officha, M. C., Okolie A. O., & Enete, I. C. (2018). Land-Use/Land-Cover Dynamics in Calabar Metropolis Using a Combined Approach of Remote Sensing and GIS. *Journal of Geographic Information System, 10,* 398-414. https://doi.org/10.4236/jgis.2018.104021

Becker, F., & Li, Z.-L. (1990). Towards a Local Split Window Method over Land Surface.

International Journal of Remote Sensing, 3, 17-33.
https://doi.org/10.1080/01431169008955028

Chen, Y. C., Chiu, H. W., Su, Y. F., Wu, Y. C., & Cheng, K. S. (2017). Does Urbanization Increase Diurnal Land Surface Temperature Variation? Evidence and Implications. *Landscape and Urban Planning, 157,* 247-258.
https://doi.org/10.1016/j.landurbplan.2016.06.014

Enete, I. C., Awuh, M. E., & Amawa, S. (2014). Assessment of Health Related Impacts of Urban Heat Island (UHI) in Douala Metropolis, Cameroon. *International Journal of Environmental Protection and Policy, 2,* 35-40.
https://doi.org/10.11648/j.ijepp.20140201.15

Enete, I. C., & Alabi, M. O. (2012). Characteristics of Urban Heat Island in Enugu during Rainy Season. *Ethiopian Journal of Environmental Studies and Management, 8,* 391-393.
https://doi.org/10.4314/ejesm.v5i4.8

Enete, I. C., & Okwu, V. U. (2013). Mapping Enugu City's Urban Heat Island. *International Journal of Environmental Protection and Policy, 1,* 50-58.
https://doi.org/10.11648/j.ijepp.20130104.12

EPA (2009). *Heat Island Compendium: Urban Heat Island Basics.*

Fabrizi, R., Bonafoni, S., & Biondi, R. (2010). Satellite and Ground-Based Sensors for the Urban Heat Island Analysis in the City of Rome. *Remote Sensing, 2,* 1400-1415.
https://doi.org/10.3390/rs2051400

Jiménez-Muñoz, J. C., Sobrino, J. A., Skoković, D., Mattar, C., & Cristóbal, J. (2014). Land Surface Temperature Retrieval Methods from Landsat-8 Thermal Infrared Sensor Data. *IEEE Geoscience and Remote Sensing Letters, 11,* 1840-1843.
https://doi.org/10.1109/LGRS.2014.2312032

Jin, M. J., Li, J. M., Wang, C. L., & Shang, R. L. (2015). A Practical Split-Window Algorithm for Retrieving Land Surface Temperature from Landsat-8 Data and a Case Study of an Urban Area in China. *Remote Sensing, 7,* 4371-4390.
https://doi.org/10.3390/rs70404371

Kurnia, E., Jaya, I. N. S., & Widiatmaka (2016). Satellite-Based Land Surface Temperature Estimation of Bogor Municipality, Indonesia. *Indonesian Journal of Electrical Engineering and Computer Science, 2,* 221-228.
https://doi.org/10.11591/ijeecs.v2.i1.pp221-228

Lin, S. P., Moore, N., Liao, L., Zhang, L., & Bengtsson, L. (2005). Analyzing Dynamic Change of Vegetation Cover of Desert Oasis Based on Remote Sensing Data in Hexi Region. In L. Bengtsson, L. Zhang, & H. Zhou (Eds.), *Proceedings of the International Symposium on Sustainable Water Resources Management and Oasis-Hydrosphere-Desert Interaction in Arid Regions* (pp. 279-295). Chinese Academy of Sciences.

Liu, L., & Zhang, Y. (2011). Urban Heat Island Analysis Using the Landsat TM Data and ASTER Data. A Case Study in Hong Kong. *Remote Sensing, 3,* 1535-1552.
https://doi.org/10.3390/rs3071535

Makinde, E. O., & Agbor, C. F. (2019). Geoinformatic Assessment of Urban Heat Island and Land Use/Cover Processes: A Case Study from Akure. *Environmental Earth Sciences, 78,* Article No. 483. https://doi.org/10.1007/s12665-019-8433-7

Mango, L. M. (2010). *Modeling the Effect of Land Use and Climate Change Scenarios on the Water Flux of the Upper Mara River Flow, Kenya.* MSc. Thesis, Florida International University.

Ofordu, C. S., Enete, I. C., & Okwu-Delunzu, V. U. (2019). Spatial and Temporal Dynamics of Land Use and Land Cover Change in Enugu, Nigeria. *African Journal of Environment, 2,* 36-39.

Oke, T. R. (1987). The Energetic Basis of the Urban Heat Island. *Quarterly Journal of Royal Meteorological Society, 108,* 1-24. https://doi.org/10.1002/qj.49710845502

Qin, Z., Karnieli, A., & Berliner, P. (2001). A Mono-Window Algorithm for Retrieving Land Surface Temperature from Landsat TM Data and Its Application to the Israel-Egypt Border Region. *International Journal of Remote Sensing, 18,* 583-594. https://doi.org/10.1080/01431160010006971

Raymond, H., & Bayarri, P. (2013). Confusion over Measures of Evidence (*p*'s) versus Errors (*α*'s) in Classical Statistical Testing. *The American Statistician, 57,* 171-178. https://doi.org/10.1198/0003130031856

Sekertekin, A., Kutoglu, S. H., & Kaya, S. (2016). Evaluation of Spatiotemporal Variability in Land Surface Temperature: A Case Study of Zonguldak, Turkey. *Environmental Monitoring and Assessment, 188,* Article No. 30. https://doi.org/10.1007/s10661-015-5032-2

Turner II, B. L., Lambin, E. F., & Reenberg, A. (2007). The Emergence of Land Change Science for Global Environmental Change and Sustainability. *Proceeding of the National Academy Sciences of the United State of America, 104,* 20666-20671. https://doi.org/10.1073/pnas.0704119104

Tyubee, B. T., & Anyadike, R. N. C. (2015). Investigating the Effects of Land Use/Land Cover on Urban Surface Temperature in Makurdi, Nigeria. *ICUC9—9th International Conference on Urban Climate Jointly with 12th Symposium on the Urban Environment.*

Usman, S. L. (2013). The Dynamic of Land Cover Change in Abuja City Federal Capital territory, Nigeria. *Confluence Journal of Environmental Studies, 8,* 14-24.

Voogt, J. A., & Oke, T. R. (2004). Thermal Remote Sensing Of Urban Climates. *Remote Sensing of Environment, 86,* 370-384. https://doi.org/10.1016/S0034-4257(03)00079-8

Wang, F., Qin, Z., Song, C., Tu, L., Karnieli, A., & Zhao, S. (2015a). An Improved Mono-Window Algorithm for Land Surface Temperature Retrieval from Landsat 8 Thermal Infrared Sensor Data. *Remote Sensing, 7,* 4268-4289. https://doi.org/10.3390/rs70404268

Wang, Y., Berardi, U., & Akbari, H. (2015b). Comparing the Effects of Urban Heat Island Mitigation Strategies for Toronto, Canada. *Energy and Buildings, 114,* 2-19. https://doi.org/10.1016/j.enbuild.2015.06.046

Weng, Q., & Fu, P. (2014). Modeling Diurnal Land Temperature Cycles over Los Angeles Using Downscaled GOES Imagery. *ISPRS Journal of Photogrammetry and Remote Sensing, 97,* 78-88. https://doi.org/10.1016/j.isprsjprs.2014.08.009

Yang, C., He, X., Yan, F., Yu, L., Bu, K., Yang, J., Chang, L., & Zhang, S. (2017). Mapping the Influence of Land Use Land Cover Changes on Urban Heat Island Effect—A Case Study of Changchun, China. *Sustainability, 9,* Article No. 312. https://doi.org/10.3390/su9020312

Yu, X., Guo, X., & Wu, Z. (2014). Land Surface Temperature Retrieval from Landsat 8 TIRS—Comparison between Radiative Transfers Equation-Based Method, Split Window Algorithm and Single Channel Method. *Remote Sensing, 6,* 9829-9852. https://doi.org/10.3390/rs6109829